Journal of Materials Chemistry A

Accepted Manuscript

ROYAL SOCIETY OF CHEMISTRY

www.rsc.org/materialsA

Journal Name

ARTICLE

The Improved Efficiency of Quantum-Dot-Sensitized Solar Cells with a Wide Spectrum and Pure Inorganic Donor-Acceptor Type Polyoxometalate as a Collaborative Cosensitizer

Received 00th January 20xx,
Accepted 00th January 20xx

DOI: 10.1039/x0xx00000x

www.rsc.org/

Li Chen,[a] Weilin Chen,[a]* Huaqiao Tan,[a]* Jiansheng Li,[b] Xiaojing Sang,[b] and Enbo Wang[a]*

Quantum dot sensitized solar cells with high theoretical conversion efficiency, low production cost and simple production process, thus received great attention in recent years. For CdSe-sensitized cells, the most significant defect of CdSe is that it has the weak absorption between 550 and 600nm and no absorption after 650nm, so it is crucial to find a wide spectrum photosensitizer to make up the defect. Here, the wide spectrum and pure inorganic Donor-Acceptor (D-A) Type Polyoxometalate (POM) $K_6H_4[a\text{-}SiW_9O_{37}Co_3(H_2O)_3]\cdot 17H_2O$ (denoted as T) is firstly introduced into the QDSCs as a collaborative cosensitizer with CdSe. The T has visible characteristic peak centering between 550 and 600nm, and after 650nm also has stronger absorption, which could make up the defect of CdSe to constitute a wide spectrum of absorption. The fluorescence spectrum, surface photovoltage spectrum, ultraviolet photoelectron spectroscopy and solid diffuse spectrum were used to explore photosensitivity of T. In addtion, the D-A Type POM can act as a good intermediate for the injection of electrons and improve the visible photocurrent response, meanwhile, it can obviously reduce the dark current and increase the electron lifetime, which can solve the problem about the high recombination at QD/ TiO_2/ electrolyte interface. In general, the best photovoltaic performance of the T and CdSe cosensitized solar cells is increased to 6.59% (J_{sc} = 18.37 mA cm^{-2}, V_{oc} = 0.57 V, *FF*= 0.63), which is improved by 32.33% compared to those of the pure CdSe-sensitized cells (J_{sc} = 16.20 mA cm^{-2}, V_{oc}= 0.50 V, *FF* = 0.61, η= 4.98%).

Introduction

Adequately developing solar energy has become the best choice to solve the energy crisis, because it is clean, accessible and long relative to other non-renewable resources.[1] For the past few years, photovoltaic cells have experienced rapid development. Since Grätzel and coworkers firstly report the dye-sensitized solar cells (DSSCs) in 1991, the highest efficiency has been up to more than 12%.[2] Quantum-dot-Sensitized solar cells (QDSCs)[3] and Perovskite solar cells[4] have also aroused wide concerns and made good achievements in recent years. Semi-conductor quantum dots, containing finite numbers of atoms, are the quasi-zero-dimensional nano-materials, which have broad application prospects in solar cells, light emitting devices, optical biomarkers, and other fields, ascribed to their quantum size effect, the band gap tunability, high absorption coefficient, solution processability, and multiple exciton generation possibilities.[5] But their low coverage on TiO_2 film, lack of panchromatic QD sensitizer, high recombination at QD/ TiO_2/ electrolyte interface, and the efficiency of electron injection hinder the improvements of power conversion efficiencies (PCE) of QDSCs. Recent years, zhong etc have come up with many new strategies to improve efficiency, and the record efficiency of QDSCs has approached 9%.[6] For CdSe-sensitized cells, the most significant defect of CdSe is that it has the weak absorption between 550 and 600nm and no absorption after 650nm, so it is crucial to find a wide spectrum photosensitizer to make up the defect.[3]

Polyoxometalates (POMs) are a class of *d*-block transitional metal oxygen clusters with remarkable structural diversity and variety of chemical compositions, which have been widely applied in optoelectronic material and devices.[7] Some transition metal-substituted POMs may absorb visible light, which can make up the shortcomings of traditional POMs only absorbing ultraviolet.[8] Recently, the transition metal-substituted POMs have been applied in the photoanodes and electrolytes of DSSCs.[9] One of the most important research part of DSSCs is the employment of pure inorganic POM-based sensitizers, which should have specific conditions: (1) the POMs should have suitable energy levels to ensure the electrons to be injected into the conduction band of titanium dioxide; (2) the POMs should not only absorb ultraviolet light, but also absorb visible light or infrared. In our previous work, we firstly explored the Keggin-type polyoxometalate $PW_{11}RhCOOH$ as the photosensitizer for assembling the POMs sensitized solar cells, and the results show that $PW_{11}RhCOOH$ displayed relatively better photovoltaic response due to energy level matching and higher

[a] Key Laboratory of Polyoxometalate Science of Ministry of Education, Department of Chemistry, Northeast Normal University, Changchun, Jilin 130024, China.
E-mail: wangeb889@nenu.edu.cn, chenwl@nenu.edu.cn, tanhq870@126.com
[b] School of Chemistry and Chemical Engineering, Liaoning Normal University, Dalian 116029, China.
†Electronic Supplementary Information (ESI) available: [details of any supplementary information available should be included here]. See DOI: 10.1039/x0xx00000x

carrier separation efficiency.[10] In addition, we purposefully investigate the energy band structures of 13 kinds of POMs according to solid diffuse reflection method and the cyclic voltammetry, and their relationship was detailed summarized and discussed.[11] Among them, T not only has the suitable level, but also has relatively wide range of spectral absorption, which can make up the defect of the visible spectral range for CdSe, so as to constitute a wide spectrum of absorption. Furthermore, the molecular orbital of T was preliminarily studied by the computational modeling, which proved that T can be regarded as a kind of donor-acceptor (D-A) type POM. Experimental result confirmed that it showed superior performance in the DSSCs.[11] So we introduce T into the QDSCs for the first time as collaborative cosensitizer to a wide spectrum of absorption.

Recent years, the collaborative cosensitization has been widely used to improve the efficiency of photovoltaic devices. From the reported literatures, a certain amount of cosensitizer added to the photovoltaic devices can improve photoresponse and charge carrier transfer, which is mainly due to the increased absorbance and the reduced recombination.[12]

Herein, T was uniformly assembled on the TiO_2 by a simple sol-gel method[13] and introduced into the QDSCs as the collaborative cosensitizer to further improve the efficiency of CdSe-sensitized QDSCs, which exhibited considerably excellent photovoltaic performance by a collaborative sensitization. The mechanism of collaborative sensitization was explained. The charge transfer process of T was proved by the Surface Photovoltage Spectroscopy (SPV) and the fluorescence emission spectrum. It is important that the T introduced into the QDSCs can reduced carrier recombination and increase the lifetime of excited electrons. Notably, different amount of T introduced into photoanodes have shown the high conversion efficiencies of 6.17%, 6.47%, 6.59% and 6.06% respectively, which are superior to that of pure CdSe-sensitized cells (4.89%).

Experimental details

Materials

$K_6H_4[\alpha\text{-}SiW_9O_{37}Co_3(H_2O)_3]\cdot 17H_2O$ was synthesized according to the report method.[14] Zinc acetate ($Zn(OAc)_2$, 99.99%), sulfur powder (99.99%), selenium powder (99.999%), oleylamine (OAm, 90%), 1-Octadecene(>90%), Oleic acid (85%) were purchased from aladdin. 3-mercaptopropionic acid (MPA, 97%) were received from J&K Chemical (Beijing, China). All other reagents were received from the Sinopharm Chemical Reagent Co., Ltd (Beijing, China) and all were used without further purification.

Synthesis of T@TiO_2

A certain amount of T was dissolved in 5 mL of deionized water formed solution A, and 5 mL Titanium isopropoxide was dropwise into the 3 mL n-butyl alcohol formed solution B. Then the solution A was added to solution B at the speed of a second every drop. The generated brown sol was dealing with 3 hours at 45 °C, and then dealing with 3 hours at 80 °C in vacuum oven. Finally, the obtained mixture was dried at 60 °C 12 hours, and 80 °C 3 hours in vacuum oven. The amount of T was 0.00 g, 0.05 g, 0.10 g, 0.20 g and 0.30 g respectively, corresponding to the T0@TiO_2, T1@TiO_2, T2@TiO_2, T3@TiO_2, T4@TiO_2.

Quantum dot sensitized solar cells fabrication

We have prepared the water-soluble 3-mercaptopropionic acid-capped CdSe quantum dot (MPA-CdSe) according to the reported method by Zhong et al.[15] The reference cells with TiO_2 photoanodes sensitized by pure CdSe were denoted as QDSCs. The pure TiO_2 paste was prepared as follows: 7.6 mL of anhydrous ethanol was added to 50 mL beaker containing 1.0 g P25 powder under ultrasonic consecutively. After sonicated for 30 min, 4.05 g of terpineol and 5.20 g of an ethanol solution with 10 wt% ethyl cellulose were added to the mixture and sonicated for another 30 min. Finally, the paste was obtained by removing ethanol through rotary evaporation method.[16] The T@TiO_2 paste was prepared as a similar method, but the only difference is that the beaker containing the mixture of 0.05 g T@TiO_2 and 0.95 g P25 powder.

We prepared the photoanode film by screen-printing the TiO_2 paste on the FTO glass. Before the screen-printing, the FTO glass had been cleaned and pretreated by 40 mmol L^{-1} $TiCl_4$ at 70 °C for 30 min. Five layers of paste were deposited on the FTO glass, each layer was treated at 120 °C for 5 min before the next layer. Then the photoanode sintered at 325 °C for 5 min, 375 °C for 5min, and 400 °C for 30 min. Subsequently, the photoanodes were treated by 40mmol L^{-1} $TiCl_4$ at 70 °C for 30 min again and sintered at 325 °C for 5 min, 375 °C for 5 min, and 400 °C for 30 min again. The prepared photoanode films were immersed to the MPA-CdSe aqueous solution for 6 hours. Subsequently, the films were rinsing with deionized water and drying with N_2. Then the photoanode films were coated with ZnS by twice dipping alternately into 0.1 M $Zn(OAc)_2$ and 0.1 M Na_2S solution for 1 min/dip.

The preparation method of polysulfide electrolyte is as follows: 0.447 g KCl, 1.928 g S, 14.414 g $Na_2S\cdot 9H_2O$ were added into the mixed solution containing 9 mL methanol and 21 mL deionized water. Then the Solution was stirring under the condition of dark overnight and filtered while being used.

Characterization

Uv-vis spectra test was investigated in the range of 200-800 nm^{-1}. TG curves were performed on a PerkinElmer TGA7 instrument at a heating rate of 10 °C min^{-1} from 30 °C to 600°C. The elemental mass ratio of W/Ti was determined by inductively coupled plasma atomic emission spectrometer (ICP-AES). X-ray powder diffraction data was collected on a Rigaku D/max-2550 diffractometer using Cu Kα radiation (λ = 1.5418Å). Fluorescence spectra were carried out with FLSP920 Fluoescence Spectrometer. The surface photovoltage spectroscopy measurement is carried out on a lab-made instrument, which constitutes a source of monochromatic light, a lock-in amplifier (SR830-DSP) with a light chopper (SR540) and a photovoltaic cell. The monochromatic light is composed of a 500 W xenon lamp (CHFXQ500 W, Global xenon lamp power) and a double-prism monochromator (Hilger and Watts, D300). The high resolution transmission electron microscope (HRTEM) (JEOL-2100F) at an acceleration voltage of 200kV and field emission scanning electron microscopy (FESEM; XL30, FEG, FEI Company) at an accelerating voltage of 25kV were used to characterize the samples. All photoelectrochemical experiments were performed on a CHI601D electrochemistry station at room temperature equipped with a Xenon lamp as the light source and an AM 1.5 solar filter.

Results and discussion

The Characterization of prepared T and CdSe

UV-vis absorption spectra of T and CdSe aqueous solution were shown in Fig. 1a to characterize the spectral range. From the Fig. 1a, CdSe has visible characteristic peak at 525 and 618 nm, and it has weak absorption between 550 and 600 nm and no absorption after 650nm. Compared with CdSe, T displayed visible characteristic peak centering between 550 and 600 nm, and after 650 nm also has stronger absorption. So T has the wide absorption in the range of visible light, which can make up the defect of the visible spectral range for CdSe. The UV-vis diffuse reflectance absorption spectra of the prepared T solid powder is shown in the Fig. 1b, from which we can draw the conclusion that the T has a strong absorption in the range of visible, and the result is consistent with UV-vis absorption spectrum of T in the Fig. 1a.

The Characterization of T@TiO_2 composites

The XRD was carried out to detect the changes of TiO_2 phase structure when the T was loaded on the surface of TiO_2. It can be seen from Fig. 2a that the location of the characteristic peaks of composites are consistent with those of anatase TiO_2 (JCPDS card No. 21-1272), which indicates that the crystal shape of TiO_2 is not changed in the T@TiO_2 composites. The UV-vis diffuse reflectance absorption spectra of T0@TiO_2, T1@TiO_2, T2@TiO_2, T3@TiO_2, T4@TiO_2 and pure TiO_2 are presented in Fig. 2b. We can see from the Fig. 2b that with the increasing of the amount of T, the absorbance of visible light of composites increased gradually, and the T0@TiO_2 and pure TiO_2 has no any absorbance in visible and infrared regions, indicating that the addition of T can increase the visible light absorption of photoanodes. The EDS analysis (Fig. S3) present the existence of W and Co elements in the composite. Elemental mapping (Fig. S4) reveals that the elements including Si, Ti, Co and W are distributed homogeneously, indicating the uniform dispersion of T on TiO_2. The oxidation states of W, Co, and Ti of T3@TiO_2 were studied by XPS (Fig. 2c, 2d and S5). The energy region of W_{4f} in T3@TiO_2 located at 35.0eV and 37.1eV are consistent with the W^{VI} oxidation state.[17] The binding energies of Co_{2p} of T3@TiO_2 show two peaks at ca.781.2eV in the energy region of $Co_{2p3/2}$ and 797.2eV in the energy region of $Co_{2p1/2}$, which are consistent with the oxidation state of Co^{II}.[18] The elemental mass ratio of W/Ti in composites were determined by ICP-AES measurement (Fig. S6), which indicates that their mass ratios are 3.78%, 7.49%, 14.17%, and 21.10%, respectively. It also well proved that the content of T assemblied on the TiO_2 was increased.

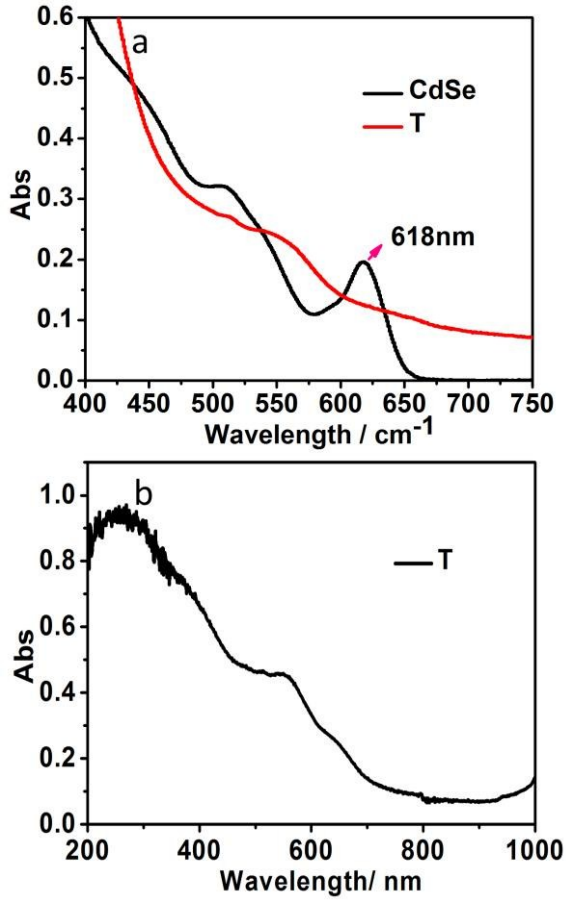

Fig. 1 a) UV-vis absorption spectrum of the the prepared T and CdSe aqueous solution; b) The UV-vis diffuse reflectance absorption spectra of the prepared T solid powder.

It can be seen from the TEM images of T3@TiO_2 composite in Fig. 3a that the interior structure of the composite is packed with nanocrystals and the surface of composite has some mesopores. The morphology of T3@TiO_2 powder was further characterized by HRTEM. In Fig. 3b, the lattice spacing of TiO_2 was measured to be 0.343nm in T3@TiO_2 powder, which can be assigned to the (101) lattice facet of anatase.[19] Additionally, many small black spots (the red circle) are scattered on TiO_2, and the size of spots are about 1.0nm, just consistent with the size of Keggin anion. The morphology of T3@TiO_2 powder was further characterized by SEM images of T3@TiO_2 (Fig. S7 and S8) indicates that the size of composite is about 150nm, and the distribution of size is relatively uniform. Besides, the SEM images of two kinds of photoanode films show that pure TiO_2 film is composed of uniform TiO_2 particles, whereas T-doped TiO_2 films contain some large particles (Fig. S9)

The Photosensitivity of T

The energy levels of T have been confirmed by the solid diffuse reflection method and the cyclic voltammetry in our previous reports (Fig. S10, S11, 4c).[11] In this work, the optical band gap was obtained through the diffuse reflectance UV-Vis spectrum for a powder sample. With reference to the literature method,[20] a plot of Kubelka-Munk function F against energy E was drawn, in which $F=(1-R)^2/2R$ and R is the reflectance of an infinitely thick layer at a given wavelength in the Fig. 4c. The band gap (E_g) is determined as the intersection point between the energy axis and the line extrapolated from the linear portion of the absorption edge in the plot of Kubelka-Munk function F against energy E_g. The E_g of T is assessed at 2.25 eV, which is smaller than TiO_2 (3.2eV). The UPS spectrum was done to obtain the position of the HOMO with respect to the vacuum level.[21] The work function (W_F) of T can be obtained around 2.37 eV (21.22-18.85) by measuring the secondary electron cut off of the photoemission spectrum. By adding the binding energy of the onset of the band of occupied orbitals, the ionization energy (I_E = 3.50 eV) of T was estimated, which gives the position of the HOMO (-2.37 eV- 3.50 eV = -5.87 eV) with respect to the vacuum level. The combination of the method of the diffuse

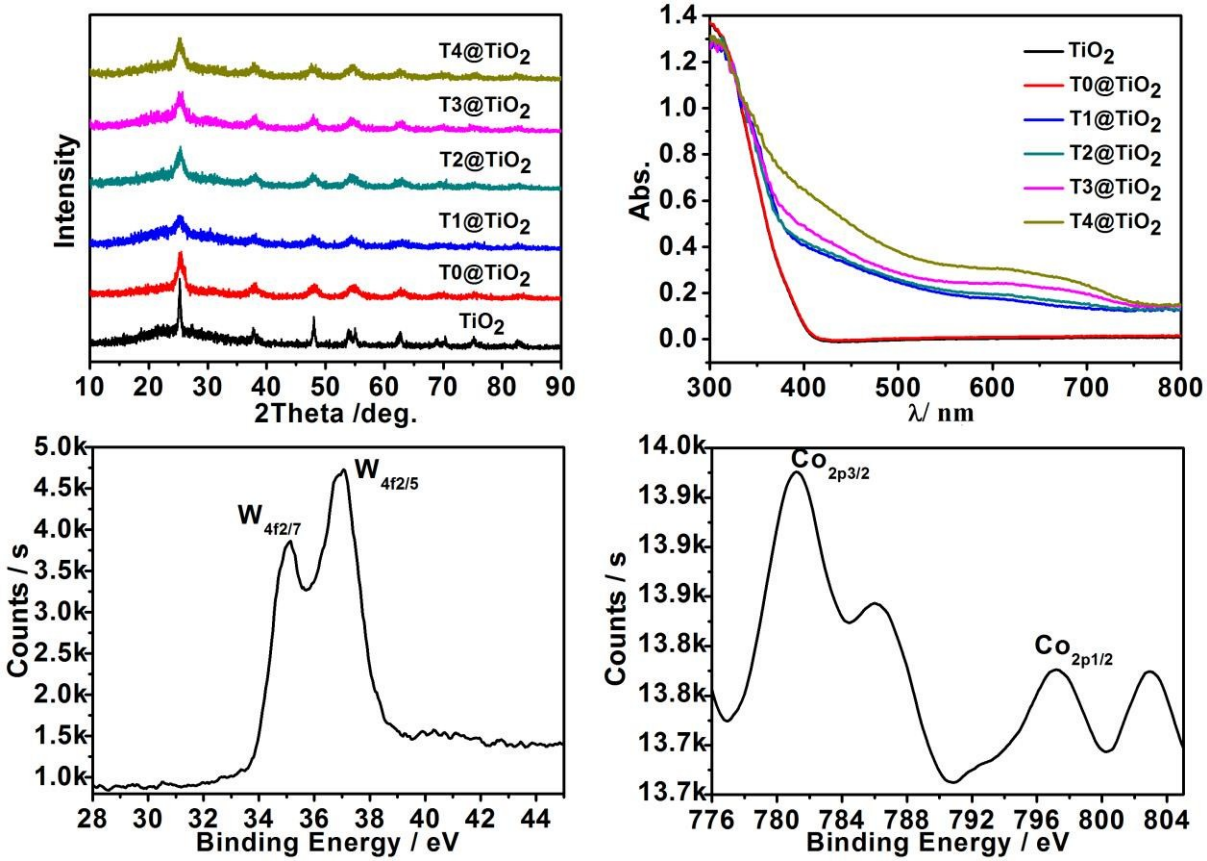

Fig. 2 a) XRD patterns of TiO_2, T0@TiO_2, T1@TiO_2, T2@TiO_2, T3@TiO_2, and T4@TiO_2; b) The UV-vis diffuse reflectance absorption spectra of T0@TiO_2, T1@TiO_2, T2@TiO_2, T3@TiO_2, T4@TiO_2 and pure TiO_2; c) and d) The X-ray photoelectron spectroscopy of W and Co of T3@TiO_2.

reflectance UV-Vis spectrum and the UPS spectrum, the LUMO level of T (-3.62eV) can be calculated.

The SPV and Fluorescence emission spectrum were used to study the charge transfer process at the interface of TiO_2 and T. The charge transfer process of T was firstly confirmed by the SPV (Fig. 4a). The SPV investigation indicates that T shows obvious light voltages at 332 nm under the condition of bias or no bias, proving that T has the nature of the semiconductor and produces effective separation of electronic-hole under the condition of light excitation.[22] The fluorescence emission spectrum was studied to further prove that electron transfer process between T and TiO_2.[23] In Fig. 4b, T has a fluorescence emission band at 360nm upon excitation at 441nm. When T was added into TiO_2 composite, the emission of T with a maximum at 360nm is very efficiently quenched by TiO_2, proving the photo-induced electron transmission from T to TiO_2.

Performance of QDSCs

The different QDSCs were assembled by fabricating different photoanodes with pure TiO_2, T1@TiO_2, T2@TiO_2, T3@TiO_2 and T4@TiO_2-doped ones combining with CdSe. The performances of the QDSCs were investigated under the simulated AM 1.5 illumination (100 mW cm^{-2}) by recording the current-voltage curves (Fig. 5a and table 1). The performance of the QDSCs with CdSe sensitized T1@TiO_2, T2@TiO_2, T3@TiO_2 and T4@TiO_2 cells were obviously enhanced compared to pure TiO_2 and T0@TiO_2 cells. The performance of the QDSCs with CdSe sensitized T0@TiO_2

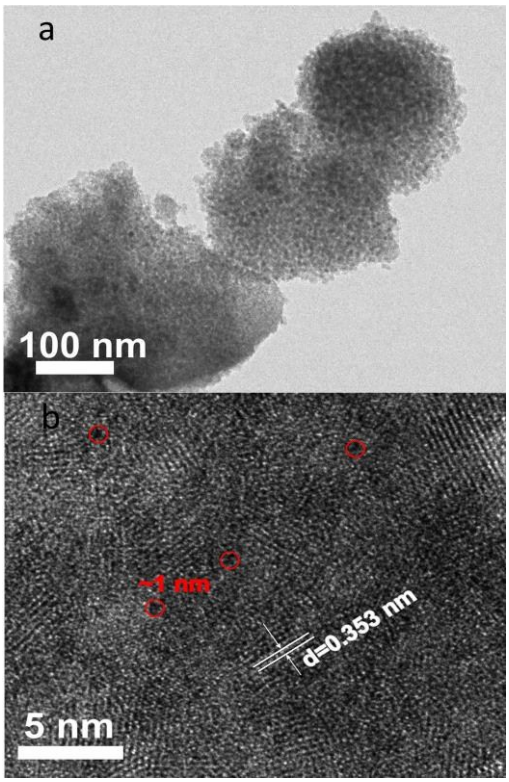

Fig. 3 a) TEM image of T3@TiO_2 powder; b) HRTEM image of T3@TiO_2 powder.

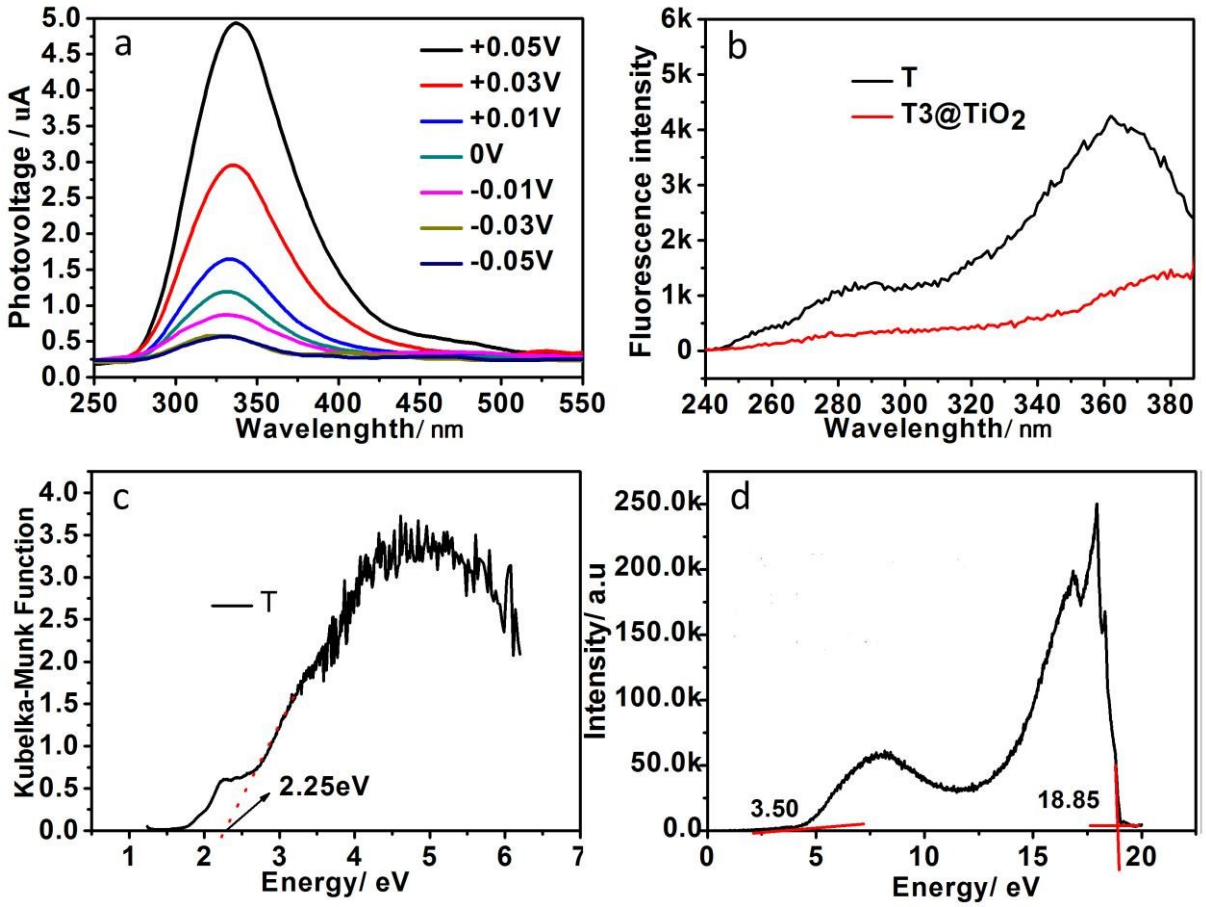

Fig. 4 a) The surface photovoltage spectroscopy of T; b) The fluorescence emission spectrum of pure TiO_2 and T2@TiO_2; c) and d) The X-ray photoelectron spectroscopy of W and Co of T3@TiO_2.

was slightly enhanced compared to pure TiO_2. The Jsc is increased from 16.20 (pure TiO_2) to 16.52 (T0@TiO_2), 17.70 (T1@TiO_2), 17.96 (T2@TiO_2), 18.37 (T3@TiO_2) and 17.56 mA cm^{-2} (T4@TiO_2). The Voc is improved from 0.50V (pure TiO_2) to 0.55V (T0@TiO_2), 0.57V (T1@TiO_2), 0.58V (T2@TiO_2), 0.57V (T3@TiO_2) and 0.56V (T4@TiO_2). The Jsc and Voc of various photoanodes increase first, then decrease with increasing the content of T. With the increasing of the amount of T, the absorption of visible light for the photoanodes is enhanced, which is the reason for the increasement of photocurrent.[11] Out the other side, the increase of Jsc results from the smoother electron transmission after the doping with T and the decrease of the dark current of QDSCs. The current voltage curves under dark condition is shown in Fig. 5c, T0@TiO_2, T1@TiO_2, T2@TiO_2, T3@TiO_2 and T4@TiO_2-doped cells can all decrease the dark current to different extents, and the dark current of T4@TiO_2-doped is no longer continue to decrease. The results show that the prepared TiO_2 particles and T can all suppress electron recombination, but effect of T was more obvious. The improvement of *Voc* is ascribed to the reduced carrier recombination occurred at the interface of FTO/ electrolyte and TiO_2/ dye/ electrolyte. The Jsc and Voc begin to decrease as the concentration continues to increase in photoanodes, demonstratin that the effect of POM on performance of QDSC is dependent on the amount of the POM.[24] The reason may come from the fact that the excessive POM will be easy to gather on the surface of titanium dioxide, which will increase the charge transfer impedance.[25] When added the concentration of T3@TiO_2 into photoanodes, the energy conversion efficiency of 6.59% was obtained.

To further investigate the enhancement of the J_{sc} value of T and CdSe cosensitized cells, the monochromatic incident photon to carrier conversion efficiency (IPCE) was used to evaluate the photocurrent response to incident light. As shown in Figure 5b, for all devices, the onset positions of the photocurrents in IPCE curves were well matched with those of the corresponding absorption spectra as shown in Fig. S13. For the CdSe sensitized pure TiO_2 and T0@TiO_2 cells, IPCE of ~68% in the range of 350-650nm were observed in the Fig. 5b. But the wider response range (350-700nm)

Table 1. Photovoltaic parameters of different QDSCs. The values of the data in the table were obtained from the average of three parallel QDSCs.

Cells	J_{sc}/ mA cm^{-2}	V_{oc}/ V	*FF*	η/ %
TiO_2	16.20	0.50	0.61	4.98±0.07
T0@TiO_2	16.52	0.55	0.56	5.10±0.05
T1@TiO_2	17.70	0.57	0.61	6.17±0.03
T2@TiO_2	17.96	0.58	0.63	6.47±0.04
T3@TiO_2	18.37	0.57	0.63	6.59±0.03
T4@TiO_2	17.56	0.56	0.62	6.06±0.05

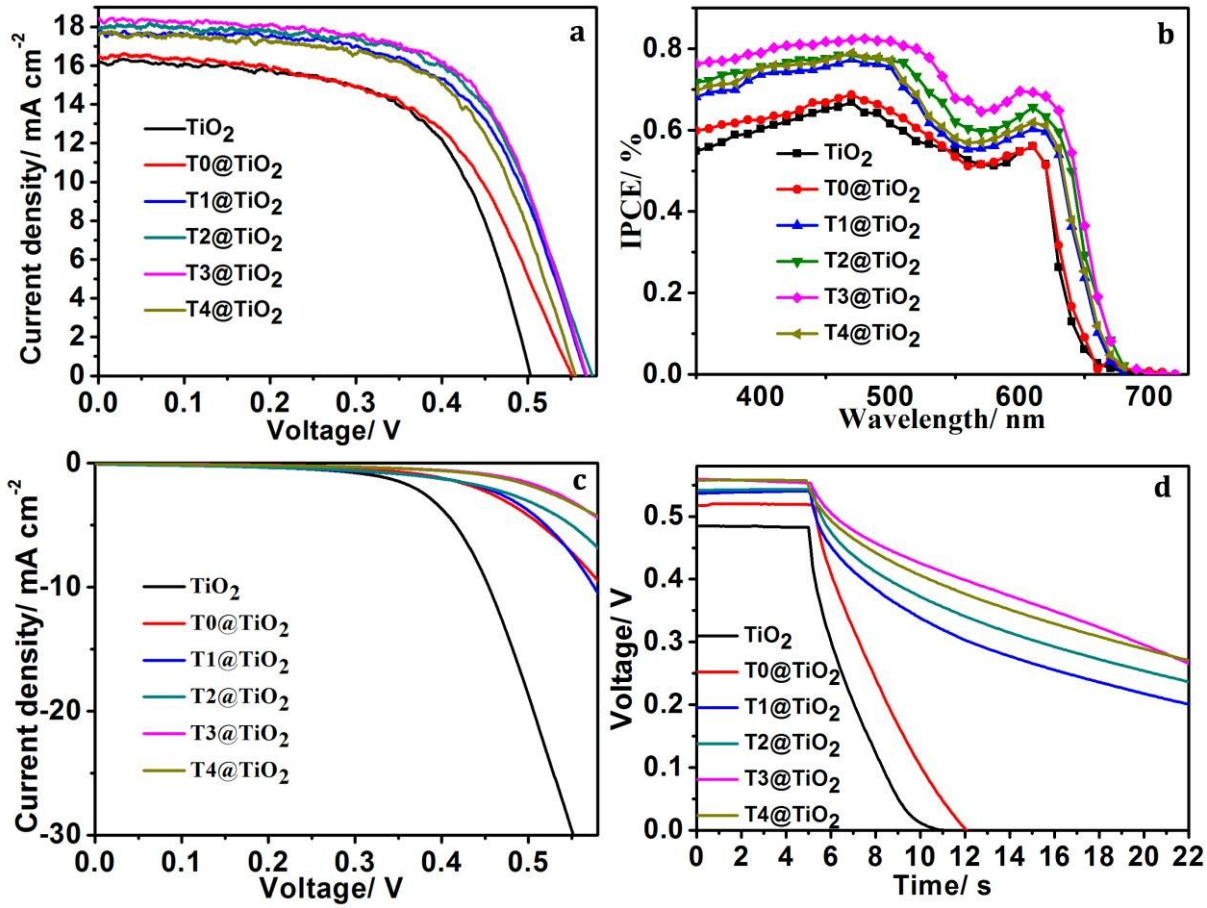

Fig. 5 a) The current-voltage curves of different QDSCs under AM 1.5 radiation (100 mW cm^{-2}); b) IPCE curves; c) Dark current curves; d) OCVD curves.

were found for CdSe sensitized T@TiO_2 (T1@TiO_2, T2@TiO_2, T3@TiO_2, T4@TiO_2) cells and the value of IPCE were ~77%, ~78%, ~83% and ~77% for CdSe sensitized T1@TiO_2, T2@TiO_2, T3@TiO_2 and T4@TiO_2 cells respectively. This can be summarized that T added to the photoanodes as collaborative cosensitizer could both utilize more sunlight and accelerate the electron transport in the photoanode. [26]

The charge separation process for the TiO_2 electrode sensitized collaboratively by T and CdSe is shown in Fig. 7. Firstly, the CdSe quantum dots would result in the electron transfer from the valence band to the conduction band under excitation of the light theoretically, thus yielding electron-hole pairs. The electron-hole pairs will produce the electron recombination or the electron transfer. While the CdSe quantum dots were sensitized collaboratively with T, the excited state photoelectrons will be injected from the conduction band of the CdSe quantum dots to the conduction band of T or TiO_2. Secondly, the electrons were collected by T and T become heteropoly blue at the same time, and soon the electrons were transferred to the conduction band of TiO_2, which can suppress the excited electron back-flow with the electrolyte or the hole of CdSe and reduce the resistance of electron injection.[27] Furthermore, most important of all is that the T owing to its smaller band gap, which was introduced to the TiO_2, can constitute a wide spectrum of absorption, so that collaborative cosensitization can produce more photoelectrons injected into the TiO_2 and improve the visible photocurrent response. T can also absorb the light and reach their excited state, and delivery the photoelectrons to the conduction band of TiO_2, which can be deduced from our previous study.[11] Such collaborative cosensitization increased visible light absorption and utilization, enhanced the spatial separation of electron-hole pairs to improve the electron injection efficiency, suppressed the electron-hole pairs recombination and therefore contributed to the final improved conversion efficiency.

Open circuit voltage decay (OCVD)

The open-circuit voltage decay (OCVD) is carried out to study the electrons recombining with the electrolytes by measuring the decay of Voc after turning off the illumination in a steady state.[28] The experimental result indicates that the introduction of T to the photoanodes results in a longer electron lifetime. Fig. 5d displays the OCVD curves of the QDSCs with T@TiO_2-doped, and pure TiO_2 photoanodes. It can be concluded from the Fig. 5d that the Voc in the QDSCs with T@TiO_2-doped photoanodes decays more slowly than that of pure TiO_2, which indicates that their charge recombination rate is much slower. The OCVD curves are further used to evaluate the electron lifetime of T@TiO_2 and pure TiO_2 photoanodes in the QDSCs by the formula $\tau_n=(kT/e)\times(dv/dt)^{-1}$. As can be seen from Fig. S12, the electron lifetime of CdSe sensitized pure TiO_2 and T0@TiO_2 cells (inset in the Fig. S12) is obviously less

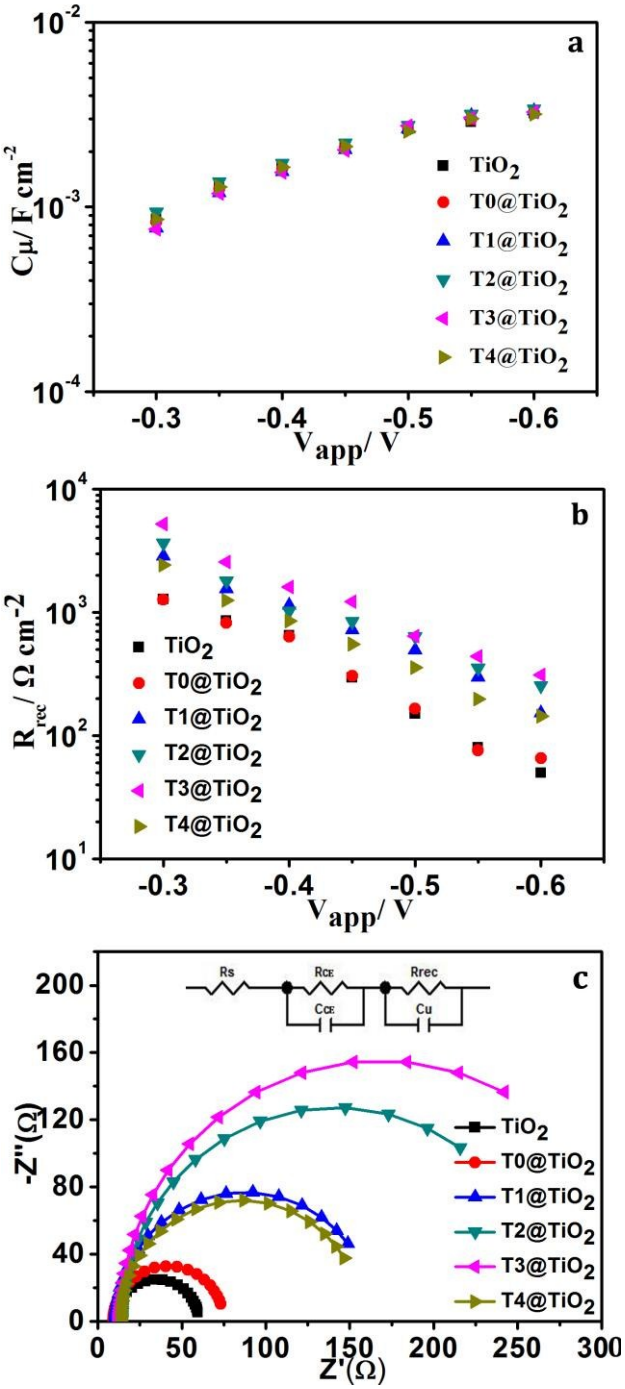

Fig. 6 Electrochemical impedance spectroscopy characterization of different QDSCs cells: (a) chemical capacitance C_{μ}, (b) recombination resistance R_{rec} and (c) Nyquist plots of cells at the forward bias of −0.60 V.

than CdSe sensitized T@TiO_2 (T1@TiO_2, T2@TiO_2, T3@TiO_2, T4@TiO_2) cells. With the increasing of the amount of T, the electron lifetime of CdSe sensitized T3@TiO_2 cells is the longest. When the amount of T continues to increase, the electron lifetime begins to shorten. This can prove that the concentration of T3@TiO_2 assembled into photoanodes is the optimal amount.

Electrochemical Impedance Spectroscopy

Electrochemical Impedance Spectroscopy (EIS) was used to investigate the intrinsic mechanism of the improved photovoltaic performance of CdSe sensitized T@TiO_2 cells.[29] Herein, the charge transmission and recombination process of CdSe sensitized T@TiO_2 and pure TiO_2 cells were evaluated by EIS, in which the different forward bias is applied in the dark with the frequency ranging from 10^5 to 0.1Hz. We can see from the Fig. 6c, the large semicircle represented the recombination resistance (R_{rec}) at the TiO_2/ QDs/ electrolyte interface and the chemical capacitance of the TiO_2 film (C_{μ}) in mid/low frequency ranges.[3f, 30] The C_{μ} mainly depicted the capability of a system to accept or release additional carriers due to a change in the Fermi level and consequently reflect the density of states.[31] The date from Nyquist plots was fitted with Zview software by using the equivalent circuit diagram in inset of Fig. 6c.

The relationship between C_{μ} or R_{rec} and the different applied bias voltages were presented in Fig. 6a and 6b. From Fig. 6a, the results showed that both CdSe sensitized T@TiO_2 and pure TiO_2 cells had nearly identical Cμ values under the same forward bias, and the T added into the photoanodes as collaborative cosensitizer did not change the conduction band edge of TiO_2 under the same forward bias.[6a] Beyond that the R_{rec} decreases with applied bias voltages increasing for all the devices in Fig. 6b. The reason was that the Fermi level of TiO_2 elevated at the forward bias is beneficial for the electron flow across the TiO_2/ QDs/ electrolyte interface.[32] From the results in Fig. 6b, there is an apparent difference in the R_{rec} values between CdSe sensitized pure TiO_2 and T@TiO_2 (T1@TiO_2, T2@TiO_2, T3@TiO_2 and T4@TiO_2) cells and the R_{rec} value of T0@TiO_2 is slightly larger than the pure TiO_2 under the identical forward bias. The R_{rec} is inversely proportional to the recombination rate, so the greater R_{rec} value means the reduced charge recombination rate.[29] The reasons are as follows: the increase of R_{rec} when the T added into the photoanodes confirmed that T plays a role in inhibiting electron recombination at the TiO_2/ QD/ electrolyte interfaces. However, continue to increase the content of T will result in the decrease of R_{rec}, which may come from the reason that the T began to gather on the surface of titanium dioxide to hinder the electronic transmission.[24,25] Besides, we find results from the experiment that the prepared TiO_2 particles are also conducive to suppress electron recombination. Fig. 6c gives a direct comparison of the CdSe sensitized T@TiO_2 and pure TiO_2 cells at a forward bias near the open-circuit voltage and the fitted data of R_{rec} and C_{μ} are listed in Table S1. From the analysis of the data in the table S1 can be concluded that the R_{rec} value of CdSe sensitized T3@TiO_2 cells

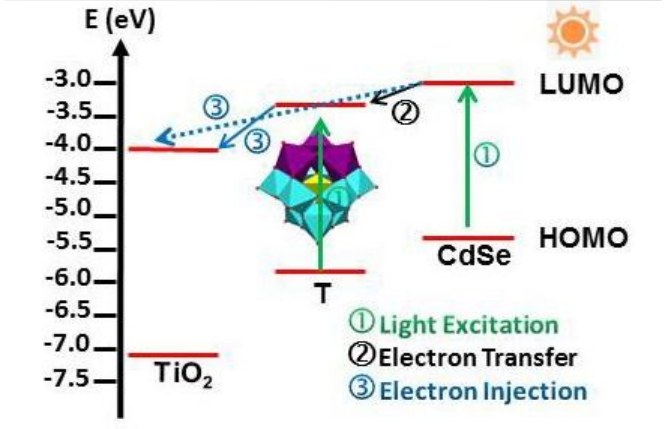

Fig. 7 The scheme of the charge separation processes for the TiO_2 electrode sensitized collaboratively by T and CdSe.

(310 Ω cm^{-2}) are higher than the CdSe sensitized pure TiO_2 cells (49 Ω cm^{-2}) and T0@TiO_2 (65 Ω cm^{-2}).

Conclusions

In conclusion, we chose a wide spectrum and pure inorganic D-A Type POM Cluster as the collaborative cosensitizer assemblied to the photoanodes of the QDSCs. The XRD, solid diffuse spectra, XPS, EDS analysis, TEM methods were used to characterize the composites, which demonstrate that T were successfully assembled on the TiO_2 and uniformly dispersed on TiO_2. The fluorescence emission spectra and the surface photovoltage spectra were used to confirm the charge transfer process between T and TiO_2. The performances of QDSCs have significant enhancements with the composites assembled in the photoanodes of the QDSCs. The overall conversion efficiency of T and CdSe cosensitized solar cells was improved by 32.33% compared to those of the pure CdSe-sensitized cells. The results show that the wide spectrum and D-A Type POM can make up the defect of CdSe QD to constitute a wide spectrum of absorption. In addition, it can act as a good intermediate for the injection of electrons and improve the visible photocurrent response, meanwhile, it can obviously reduce the dark current and increase the electron lifetime. More importantly, the present work takes the first step for using D-A Type POM as the potential substitutes for dyes of high efficiency QDSCs. Further studies about D-A Type POMs are in progress.

Acknowledgment

This work was financially supported by the National Natural Science Foundation of China (No. 21131001 and 21201031), the Open Subject Foundation of Key Laboratory of Polyoxometalate Science of Ministry of Education, the open research fund program of the State Key Laboratory of Luminescence and Applications (Changchun Institute of Optics, Fine Mechanics and Physics, CAS), the Science and Technology Research Foundation of the Thirteenth Five Years of Jilin Educational Committee (No. [2015]542), the Technology Foundation for Selected Overseas Chinese Scholars of Personnel Ministry of China, and the Analysis and Testing Foundation of Northeast Normal University.

Notes and references

1 (a) J. Liu, Y. Liu, N. Y. Liu, Y. Z. Han, X. Zhang, H. Huang, Y. Lifshitz, S.-T. Lee, J. Zhong, Z. H. Kang, *Science*, 2015, **347**, 970-974; (b) M. Z. Yu, W. D. McCulloch, D. R. Beauchamp, Z. J. Huang, X. D. Ren, and Y. Y. Wu, *J. Am. Chem. Soc*, 2015, **137**, 8332-8335; (c) H. Wang , J. T. Yang , X. l. Li , H. Z. Zhang , J. H. Li , and L. Guo, *small*, 2012, **8**, 2802–2806.

2 (a) B. O'Regan and M. Grätzel, *Nature*, 1991, **353**, 737-740; (b) A. Yella, H. W. Lee, H. N. Tsao, C. Yi, A. K. Chandiran, M. K. Nazeeruddin, E. W. G. Diau, C. Y. Yeh, S. M. Zakeeruddin and M. Grätzel, *Science*, 2011, **334**, 629-634. (c) M. Grätzel, R. A. J. Janssen, D. B. Mitzi and E. H. Sargent, *Nature*, 2012, **488**, 304.

3 (a) V. G. Pedro, X. Xu, I. M. Seró, and J. Bisquert, *ACS Nano*, 2010, **4**, 5783-5790; (b) P. K. Santra and P. V. Kamat, *J. Am. Chem. Soc*, 2012, **134**, 2508-2511; (c) X. M. Huang, S. Q. Huang, Q. X. Zhang, X. Z. Guo, D. M. Li, Y. H. Luo, Q. Shen, T. Toyoda and Q. B Meng, *Chem. Commu*, 2011, **47**, 2664-2666; (d) S. M. Wang, W. W. Dong, R. H. Tao, Z. H. Deng, J. Z. Shao, L. H. Hu, J. Zhu, X. D. Fang, *Journal of Power Sources*, 2013, **235**, 193-201; (e) P. K. Santra and P. V. Kamat. *J. Am. Chem. Soc*. 2013, **135**, 877-885; (f) J. Wang, I. M. Seró, Z. X. Pan, K. Zhao, H. Zhang, Y. Y. Feng, G. Yang, X. H. Zhong, and J. Bisquert, *J. Am. Chem. Soc*. 2013, **135**, 15913-15922; (g) K. Zhao, Z. X. Pan, I. M.-Seró, E. Canovas, ì H. Wang, Y. Song, X. Q. Gong, M. Bonn, J. Bisquert and X. H. Zhong, *J. Am. Chem. Soc*. 2015, **137**, 5602-5609.

4 W. S. Yang, J. H. Noh, N. J. Jeon, Y. C. Kim, S. C. Ryu, J. W. Seo, S. Il. Seok, *science*, 2015, **348**, 1234-1237. (b) M. Grätzel. *Nat. Mater*. 2014, **13**, 838. (c) M. M. Lee, J. Teuscher, T. Miyasaka, T. N. Murakami, H. J. Snaith, *Science*, 2012, **338**, 643. (d) M. Liu, M. B. Johnston, H. J. Snaith, *Nature,* 2013, **501**, 395.

5 (a) Y. Q. Li, A. Rizzo, R. Cingolani, G. Gigli, Adv. Mater. 2006, **18**, 2545-2548; (b) W. C. W. Chan, D. J. Maxwell, X. H. Gao, R. E. Bailey, M. Y. Hanc, S. M. Nie, *Current Opinion in Biotechnology*, 2002, **13**, 40-46; (c) V. Ryzhii, *Semiconductor Science and Technology*, 1996, **11**, 759-765.

6 (a) Z. W. Ren, J. Wang, Z. X. Pan, K. Zhao, H. Zhang, Y. Li, Y. X. Zhao, I. M.-Sero, J. Bisquert and X. H. Zhong, *Chem. Mater.*, 2015, **27**, 8398−8405; (b) J. Wang, Y. Li, Q. Shen, T. Izuishi, Z. X. Pan, K. Zhao and X. H. Zhong, J. Mater. Chem. A, 2016, 4, 877–886; (d) S. Jiao, Q. Shen, I. M.-Sero, J. Wang, Z. X. Pan, K. Zhao, Y. K. Kuga, X. H. Zhong and J. Bisquert, ACS Nano, 2015, 9, 908-915.

7 (a) A. Müller, M. T. Pope, F. Peters, D. Gatteschi, *Chem. Rev*, 1998, **98**, 239-271; (b) M. T. Pope, A. Müller, *Angew. Chem. Int. Ed*, 1991, **30**, 34-48; (c) F. P. Xiao, J. Hao, J. Zhang, C. L. Lv, P. C. Yin, L. S. Wang and Y. G. Wei, *J. Am. Chem. Soc*, 2010, **132**, 5956-5957; (d) L. Chen, J. Y. Guo, X. Xu, W. W. Ju, D. Zhang, D. R. Zhu and Y. Xu, *Chem. Commun*., 2013, **49**, 9728-9730.

8 (a) C. L. Hill, C. M. P. McCartha, *Coordination Chemistry Reviews*, 1995, **143**, 407-455; (b) J. W. Zhao, J. Zhang, S. T. Zheng , and G. Y. Yang, *Inorg. Chem*, 2007, **46**, 10944-10946.

9 (a) S. S. Xu, W. L. Chen, Y. H. Wang, Y. G. Li, Z. J. Liu, C. H. Shan, Z. M. Su and E. B. Wang, *Dalton Trans.*, 2015, **44**, 18553-18562; (b) X. J. Sang, J. S. Li, L. C. Zhang, Z. M. Zhu, W. L. Chen, Y. G. Li, Z. M. Su and E. B. Wang, *Chem. Commun*., 2014, **50**, 14678-14681; (c) C. C. Yuan, S. M. Wang, W. L. Chen, L. Liu, C. Qin, Z. M. Su and E. B. Wang, *Dalton Tran.*, 2014, **43**, 1493-1497; (d) L. Chen, X. J. Sang, J. S. Li, C. H. Shan, W. L. Chen, Z. M. Su, E. B. Wang, *Inorganic Chemistry Communications.*, 2014, **47**, 138-143.

10 J. S. Li, X. J. Sang, W. L. Chen, L. C. Zhang, Z. M. Su, C. Qin, E. B. Wang, *Inorganic Chemistry Communications.*, 2013, **38**, 78–82.

11 J. S. Li, X. J. Sang, W. L. Chen, L. C. Zhang, Z. M. Zhu, T. Y. Ma, Z. M. Su, and E. B. Wang, *ACS Appl. Mater. Interfaces*, 2015, **7**, 13714-13721.

12 (a) Y. Q. Wang, B. Chen, W. J. Wu, X. Li, W. H. Zhu, H. Tian and Y. S. Xie, *Angew. Chem. Int. Ed.*, 2014, **53**, 10779-10783; (b) C. Chen, G. Ali, S. H. Yoo, J. M. Kuma and S. O. Cho, *J. Mater. Chem.*, 2011, **21**, 16430; (c) M. Seol, H. J. Kim, W. S. Kim, K. J. Yong, *Electrochemistry Communications.,* 2010, **12**, 1416-1418.

13 L. Li, Y. L. Yang, R. Q. Fan, *Dalton Trans*, 2014, **43**, 1577-1582.

14 J. F. Liu, F. Ortega, P. Sethuraman, D. E. Katsoulis, C. E. Costello and M. T. Pope, *J . CHEM. SOC. DALTON TRANS.*, 1992, 1901-1906.

15 H. Zhang, K. Cheng, Y. M. Hou, Z. Fang, Z. X. Pan, W. J. Wu, J. L. Hua and X. H. Zhong, *Chem. Commun.*, 2012, **48**, 11235-11237.

16 Z. L. Du, H. Zhang, H. L. Bao and X. H. Zhong, *J. Mater. Chem. A*, 2014, **2**, 13033-13040.
17 K. T. Ng, D. M. Hercules, *J. Phys. Chem*., 1976, **80**, 2094-2102.
18 X. Chen, Y. C. Dai, Z. B. Zheng, K. Z. Wang, *J. Colloid Interface Sci.*, 2013, **402**, 107-113.
19 Q. Zhu, J. S. Qian, H. Pan, L. Tu and X. F. Zhou, *Nanotechnology*, 2011, **22**, 395703.
20 A. Hiskia, A. Mylonas and E. Papaconstantinou, *Chem. Soc. Rev.*, 2001, **30**, 62-69.
21 M. Vasilopoulou, A. M. Douvas, L. C. Palilis, S. Kennou,and P. Argitis, *J. Am. Chem. Soc*., 2015, **137**, 6844−6856.
22 X. Luo, F. Li, B. Xu, Z. Sun, L. Xu, *J. Mater. Chem*., 2012, **22**, 15050-15055.
23 J. Desilvestro, M. Grätzel, L. Kavan, J. Moser, J. Augustynski, *J. Am. Chem. Soc*, 1985, **107**, 2988-2990.
24 A. Dolbecqa, P. Mialanea, B. Keitab and L. Nadjo, *J. Mater. Chem.*, 2012, **22**, 24509-24521.
25 A. Dolbecqa, P. Mialanea, B. Keitab and L. Nadjo, *J. Mater. Chem.*, 2012, **22**, 24509-24521.
26 (a) X. J. Sang, J. S. Li, L. C. Zhang, Z. J. Wang, W. L. Chen, Z. M. Zhu, Z. M. Su and E. B. Wang, *ACS Appl. Mater. Interfaces*, 2014, **6**, 7876−7884; (b) Y. X. Jiang, Y. L. Yang, L. S. Qiang, R. Q. Fan, H. P. Ning, L. Li, T. L. Ye, B. Yang, W. W. Cao, *Journal of Power Sources*, 2015, **278**, 527–533.
27 S. M. Wang, L. Liu , W. L. Chen, E. B. Wang and Z. M. Su, *Dalton Trans.*, 2013, **42**, 2691-2695.
28 (a) J. Bisquert, A. Zaban, M. Greenshtein, I. M. Seró, *J. Am. Chem. Soc*, 2004, **126**, 13550-13559; (b) A. Zaban, M. Greenshtein and J. Bisquert, *Chemphyschem*, 2003, **4**, 859.
29 F. F.-Santiago, G. G.-Belmonte, I. M.-Seró and J. Bisquert, *Phys. Chem. Chem. Phys.,* 2011, **13**, 9083-9118.
30 I. M.-Seró, S. Giménez, F. F.-Santiago, R. Gómez, Q. Shen, T. Toyoda and J. Bisquert, *Acc. Chem. Res.*, 2009, **42**, 1848–1857.
31 M. A. Hossain, J. R. Jennings, C. Shen, J. H. Pan, Z. Y. Koh, N. Mathews and Q. Wang, *J. Mater. Chem.*, 2012, **22**, 16235-16242.
32 G. S. Wang, H. Y. Wei, Y. H. Luo, H. J. Wu, D. M. Li, X. H. Zhong, Q. B. Meng, *Journal of Power Sources*, 2016, **302**, 266-273.

Journal Name

ARTICLE

The Improved Efficiency of Quantum-Dot-Sensitized Solar Cells with a Wide Spectrum and Pure Inorganic Donor-Acceptor Type Polyoxometalate as a Collaborative Cosensitizer

Received 00th January 20xx,
Accepted 00th January 20xx

DOI: 10.1039/x0xx00000x

www.rsc.org/

Li Chen,[a] Weilin Chen,[a*] Huaqiao Tan, [a*] Jiansheng Li,[b] Xiaojing Sang,[b] and Enbo Wang[a*]

The wide spectrum and pure inorganic Donor-Acceptor type polyoxometalate was assemblied on the TiO_2 as the collaborative cosensitizer of QDSCs, which tremendously improved the performance of the QDSCs to be 6.59%.

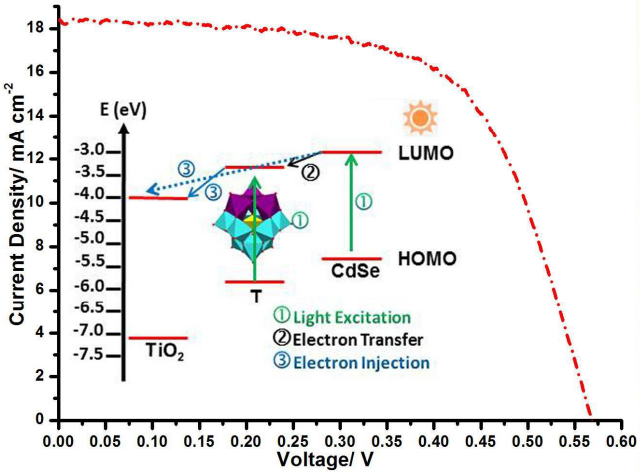

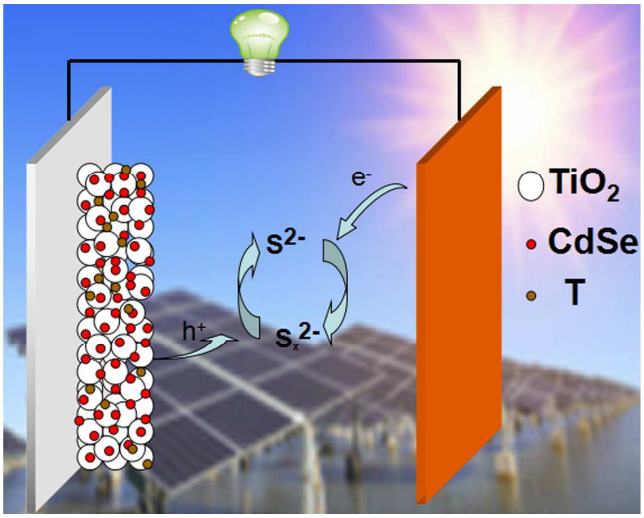

[a] Key Laboratory of Polyoxometalate Science of Ministry of Education, Department of Chemistry, Northeast Normal University, Changchun, Jilin 130024, China. E-mail: wangeb889@nenu.edu.cn, chenwl@nenu.edu.cn

[b] School of Chemistry and Chemical Engineering, Liaoning Normal University, Dalian 116029, China.

†Electronic Supplementary Information (ESI) available: [details of any supplementary information available should be included here]. See DOI: 10.1039/x0xx00000x